STING deficiency-associated aberrant CXCL10 expression contributes to pathogenesis of arthritogenic alphaviruses

Tao Lin[1*], Tingting Geng[1*], Andrew Harrison[1], Duomeng Yang[1], Anthony T. Vella[1], Erol Fikrig[2], Penghua Wang[1]

[1] Department of Immunology, School of Medicine, University of Connecticut Health Center, Farmington, CT 06030, USA.

[2] Section of Infectious Diseases, School of Medicine, Yale University, New Haven, CT06520, USA.

* These authors contributed equally

Address correspondence to: Penghua Wang, Ph.D., Department of Immunology, School of Medicine, University of Connecticut Health Center, Farmington, CT 06030, USA. Email: pewang@uchc.edu, Tel: 860-679-6393

Running title: A role of CXCL10 in pathogenesis of alphaviral arthritis

Abstract

Arthritogenic alphaviruses such as Chikungunya virus and O'nyong nyong virus cause acute and chronic crippling arthralgia associated with inflammatory immune responses. However, the physiological functions of individual immune signaling pathways in the pathogenesis of alphaviral arthritis remain poorly understood. Here we report that a deficiency in the stimulator-of-interferon-genes (STING) led to enhanced viral loads, exacerbated inflammation and selectively elevated expression of CXCL10, a chemoattractant for monocytes/macrophages/T cells, in mouse feet. *Cxcl10*$^{-/-}$ mice had the same viremia as wild-type animals, but fewer immune infiltrates and lower viral loads in footpads at the peak of arthritic disease (6-8 days post infection). Macrophages constituted the largest immune cell population in footpads following infection, which were significantly reduced in *Cxcl10*$^{-/-}$ mice. The viral RNA loads in neutrophils and macrophages were reduced in *Cxcl10*$^{-/-}$ compared to wild-type mice. In summary, our results demonstrate that STING signaling represses, while CXCL10 signaling promotes, pathogenesis of alphaviral disease.

Key words: STING**,** CXCL10, alphavirus, Chikungunya, viral arthritis

Introduction

Alphaviruses are a genus of single-stranded positive sense RNA viruses within the *Togaviridae* family. These viruses are mainly transmitted by mosquitoes and pose a public health threat worldwide, particularly in tropical/subtropical regions. Many alphaviruses are arthritogenic, including Chikungunya (CHIKV), O'nyong-nyong (ONNV) and Ross River viruses (RRV) *etc*. CHIKV is the causative agent of acute and chronic crippling arthralgia that was initially identified in Tanzania in 1952 [1]. Since then, several major epidemics have been recorded on the Indian Ocean islands, India, Southeast Asia, which resulted in over 6 million cases [2]. In late 2013, CHIKV emerged on the Caribbean islands, and has now spread to more than 50 countries across the Central and South America, including autochthonous infections in the United States and caused over 2.5 million infection cases (Sources: Pan America Health Organization). Approximately 50% of CHIKV-infected patients suffer from rheumatic manifestations that last 6 months to years, with ~5% of the victims having rheumatoid arthritis-like illnesses [3,4].

During the acute phase of infection in humans (~ two weeks), CHIKV infects many organs and cell types [2], induces apoptosis and direct tissue damage [5-7]. The acute phase is also characteristic of robust innate immune responses, including high levels of type I IFNs, proinflammatory cytokines/chemokines and growth factors [5,8-12]. Immune cell infiltration is a hallmark of acute CHIKV infection, including primarily macrophages, monocytes, but also neutrophils, dendritic cells, NK cells and lymphocytes [2]. In the chronic phase, CHIKV arthritis may progress without active viral replication, typified by elevated expression of cytokines and immune cell infiltration [2,13]. In particular, human arthritic disease severity is associated with a high level of serum chemoattractants for monocytes/macrophages/T cells, CXCL10 and CXCL9 [14]. In mice, CHIKV infection leads to a low viremia lasting usually 5-7 days, which is limited by type I IFNs [11,15-17] and is subsequently cleared by virus-specific antibody responses [18-25]. When inoculated directly into a mouse foot pad, CHIKV elicits overt arthritic symptoms including the first peak of foot swelling characteristic of edema occurring 2-3 days post infection and a second

peak at 6-8 days post infection [26] with massive infiltration of immune cells into infected feet [16,27-32].

The stimulator of interferon genes (STING) participates in innate immunity to both DNA and RNA viruses. During DNA virus infections, STING signaling induces type I interferons (IFNs) after being engaged by a second messenger cyclic GMP-AMP (cGAMP), which is synthesized by a viral DNA receptor, cGAMP synthase (cGAS) [33-38 39 40]. Our study with West Nile virus (WNV) and other recent studies conclusively demonstrate that STING is also important for the control of RNA virus infection in mouse models [33,41-43]; likely through upregulation of type I IFNs [33 44 45], induction of a specific set of chemokines via Signal Transducer and Activator of Transcription 6 (STAT6) [43], translation inhibition of viral gene expression [46] and/or other unknown mechanisms. Intriguingly, STING signaling was recently shown to induce expression of negative regulators of innate immune signaling, such as suppressor of cytokine signaling (SOCS), to control Toll-like receptor (TLR)-mediated hyper inflammatory immune responses in a lupus mouse model [47]. We herein report that a deficiency in the stimulator-of-interferon-genes (STING) led to enhanced viral loads, exacerbated inflammation and selectively elevated expression of CXCL10 in mouse feet. *Cxcl10*$^{-/-}$ mice had the same viremia as wild-type animals, but fewer immune infiltrates and lower viral loads in footpads at the peak of arthritic disease (days 6-8 post infection). Macrophages constituted the largest immune cell population in footpads following infection, which were significantly reduced in *Cxcl10*$^{-/-}$ mice. The viral RNA loads in neutrophils and macrophages were also reduced in *Cxcl10*$^{-/-}$ compared to wild-type mice.

Results

A STING deficiency leads to enhanced viral loads, exacerbated inflammation and selectively elevated expression of CXCL10

STING signaling is essential for induction of immune responses to DNA viruses. Our studies with West Nile virus (WNV) and other recent studies conclusively demonstrated that STING is also important for the control of RNA virus infection in mouse models [33,41-43]. This is also observed with CHIKV infection (**Fig. 1**). When inoculated directly into a mouse footpad, CHIKV elicits a brief viremia that lasts ~ 5 days and overt arthritic symptoms including the first peak of foot swelling characteristic of edema occurring 2-3 days post infection and a second peak at 6-8 days post infection [26] with massive infiltration of immune cells into infected feet [16,27-32]. Sting-deficient mice (*Sting*$^{gt/gt}$) [48] presented a significant increase in viremia from 12hrs through 96hrs post infection (p.i.) compared to wild-type (WT mice) (**Fig.1 A, B**). Furthermore, the viral loads in the spleen were much higher in *Sting*$^{gt/gt}$ than WT mice too (**Fig.1 C**). The viral loads in the feet were elevated at day 4 p.i. in *Sting*$^{gt/gt}$ compared to WT mice; however, this difference disappeared by day 6 and 8 p.i. (**Fig.1 D, E**). *Sting*$^{gt/gt}$ mice showed much greater footpad swelling from days 4 through 8 p.i., than WT mice (**Fig.1 F**). Histopathology analysis by Haemotoxylin and Eosin (H&E) staining demonstrated a significant increase of immune cells in muscle/synovial cavity/tendon in *Sting*$^{gt/gt}$ compared to WT mice (**Fig.1 G, H**). Interestingly, although the viral loads in *Sting*$^{gt/gt}$ joints were the same as WT at days 6 and 8 after infection (**Fig.1 D**), the joint disease manifestations were much more severe in *Sting*$^{gt/gt}$ (**Fig.1 F-H**).

Since immune cell infiltration into joints and muscles is a hallmark of CHIKV arthritis, we examined chemoattractant expression in mouse ankle joints. A chemokine PCR array was performed with joint samples at the peak of disease (day 8 p.i). Two genes *Ifng* and *Cxcl10* (also known as IFN-γ inducible gene-IP10) were upregulated by 4-5 fold and three genes (*Cxcl5*, *Cxcr2*, *Ppbp*) were down-regulated by over 3 fold in *Sting*$^{gt/gt}$ compared to WT mice (**Fig.2 A**). Downregulation of *Cxcl5* is consistent with upregulation of IFN-γ, as Cxcl5 can be inhibited by IFN-γ [49]. Cxcl10 is a chemoattractant for T cells, monocytes/macrophages, natural killer cells (NKs), and dendritic cells (DCs); Cxcl5, Cxcr2, and Ppbp (also known as Cxcl7) participate in neutrophil recruitment. We next validated the PCR array results and investigated the kinetics of

chemokine expression during the course of CHIKV infection. In WT mouse joints, *Ifng* and *Cxcl10* mRNA expression was continuously upregulated by ~7-10-fold, and further elevated in *Sting*$^{gt/gt}$ mice at days 4 through 8 p.i. (**Fig.2 B**), coincidently with arthritis progression. *Ppbp* expression was equally upregulated in both WT and *Sting*$^{gt/gt}$ mice at day 4 p.i., but rapidly decreased at day 8 p.i. in *Sting*$^{gt/gt}$ mice (**Fig.2 B**). Ccl5 (a chemoattractant for T cells, eosinophils and basophils) and Ccl1 (chemoattractant for monocytes), Ccl20 (strongly chemotactic for lymphocytes), Ccl26 (chemotactic for eosinophils and basophils) were transiently up-regulated at day 4 p.i. and down-regulated at day 8 p.i. similarly in both WT and *Sting*$^{gt/gt}$ mice (**Fig.2 B**). These data demonstrate that IFN-γ and CXCL10 expression kinetics are in line with arthritis progression and suggest a role for IFN-γ and CXCL10 in disease pathogenesis. However, IFN-γ has been known to play an anti-CHIKV role [50] and thus is excluded for further investigation.

CXCL10 signaling contributes to alphavirus pathogenesis

To investigate the physiological role of CXCL10 in alphavirus pathogenesis, we inoculated CHIKV directly into the footpads of both wild-type (WT) and Cxcl10 knockout (*Cxcl10*$^{-/-}$) mice. The results show that the viremia of *Cxcl10*$^{-/-}$ mice were comparable to those in WT mice at days 2 and 4 p.i. (**Fig.3 A**), suggesting that CXCL10 is dispensable for controlling systemic dissemination of CHIKV. The viral loads in the infected feet of WT and *Cxcl10*$^{-/-}$ mice were the same at day 2 p.i., increased modestly in WT at day 4 p.i., while dropped significantly and rapidly in *Cxcl10*$^{-/-}$ mice from days 4 through 7 (**Fig.3 B**), suggesting that CXCL10 signaling promotes viral persistence. Intriguingly, histopathological analyses by H&E staining confirmed a moderate decrease in immune cell numbers in the muscles and joints of *Cxcl10*$^{-/-}$ compared to WT mice (**Fig.3 C**). Consistently, the mRNA expression of *Ifnb1* and inflammatory cytokines (*Il6*, *Tnfa*) was reduced in *Cxcl10*$^{-/-}$ joints at day 7 p.i. compared to WT (**Fig.3 D**). We next asked if this phenomenon is applicable to other arthritogenic viruses. To this end, we chose O'nyong-

nyong (ONNV), which together with CHIKV are members of the Semliki Forest antigenic complex of the *Alphavirus* genus. Consistent with the results from CHIKV studies, ONNV viremia were not influenced by *Cxcl10* deficiency (**Fig.4 A**); while the viral loads in the infected feet were lower in *Cxcl10*$^{-/-}$ than those in WT mice at day 6 p.i. (**Fig.4 B**). Histopathological analyses (arbitrary score) by hematoxylin and eosin staining confirmed a moderate decrease in immune cell infiltration into the muscles and joints of *Cxcl10*$^{-/-}$ compared to WT mice (**Fig.4 C**). These data suggest that CXCL10 signaling promotes alphaviral persistence and immune cell infiltration into mouse feet.

CXCL10 signaling promotes macrophage recruitment to infected feet

Since CXCL10 is a chemoattractant for monocytes/macrophages, we analyzed the immune infiltrates in the infected feet by fluorescence activated cell sorting (FACS) to identify and quantitate individual cell populations. In WT mice, total CD45^{+} cells increased modestly at day 2 p.i., decreased a bit at day 4 p.i. and went up again at day 6 p.i. There was a modest decrease in CD45^{+} cells in *Cxcl10*$^{-/-}$ at day 6 p.i. compared to WT (P=0.06) (**Fig.5 A**). Macrophages were recruited rapidly as early as day 2 p.i. and were the largest immune population at all the censored time points. Intriguingly, these cells were significantly fewer in *Cxcl10*$^{-/-}$ than WT mice at day 6 p.i. (**Fig.5 B**). Neutrophils constituted the second largest immune population and infiltrated into the infected feet similarly between WT and *Cxcl10*$^{-/-}$ mice in terms of quantities and kinetics (**Fig.5 C**). Compared to those in the uninfected mice (day 0), the numbers of conventional dendritic cells (cDC) were only significantly increased by day 6 p.i. and higher in *Cxcl10*$^{-/-}$ than WT mice (**Fig.5 D**). Plasmacytoid dendritic cells (pDC) were also recruited to the infected feet as early as day 2 p.i. and their numbers were the same in both genotypes (**Fig.5 E**).

CXCL10 signaling promotes alphavirus persistence in infiltrating neutrophils and macrophages

The abovementioned data show that macrophages and neutrophils are the primary infiltrating cells in the infected mouse feet, and interestingly the former has been demonstrated to be likely a source of CHIKV persistence in nonhuman primates [51]. We then examined ONNV RNA loads in each cell population after FACS. We were able to extract RNA from paraformaldehyde-fixed cells using a specialized RNA kit and quantitated viral RNA by qRT-PCR. Among all immune cells, neutrophils contained the highest viral load, which was dramatically reduced in *Cxcl10*$^{-/-}$ mice (P=0.03) compared to WT mice (**Fig.6**). Macrophages had the second highest viral load, which was also decreased in *Cxcl10*$^{-/-}$ (P=0.05). The viral loads in cDC and pDC, though at a much lower level than neutrophil/macrophages, trended lower in *Cxcl10*$^{-/-}$ (**Fig.6**). These data suggest that during the acute phase of infection neutrophils and macrophages are likely an important source of alphaviral replication in infected tissues, and CXCL10 signaling promotes alphavirus persistence in infiltrating neutrophils and macrophages in the foot.

Discussion

Many studies including ours have firmly established that STING signaling plays a critical anti-RNA virus role [33,41-43], likely by multiple mechanism including, but not limited to, induction of type I IFNs [33 44 45], a specific set of chemokines via STAT6 [43], and translation inhibition of viral gene expression [46]. In agreement with these published studies, this study shows that STING signaling is also critical for controlling alphavirus infection in mice. Intriguingly, exacerbated pathology progressed in Sting-deficient mouse feet even when viral loads were repressed to similarly low levels between WT and Sting-deficient mice at days 6 and 8 p.i. (**Fig.1 D-H**). These results are in agreement with previous observations showing that CHIKV arthritis severity is not always positively correlated with viral loads [28], but rather is a primary consequence of dysregulated inflammatory responses. Thus, our data suggest that STING signaling may not only limit viral replication at the early stage, but also keep aberrant inflammatory responses in check to avoid

immunopathology at the later stage. Indeed, STING signaling was recently shown to induce expression of negative regulators of innate immune signaling, such as suppressor of cytokine signaling (SOCS), to control Toll-like receptor (TLR)-mediated hyper inflammatory immune responses in a lupus mouse model [47]. Plasmacytoid DCs (pDCs) that express a very high level of TLR7 (a viral RNA sensor) was the most rapidly and highly expanded cell type in mouse feet on day 7 after CHIKV/ONNV infection compared to non-infected (**Fig.5 E**) [52].

CXCL10 is a chemoattractant for monocytes/macrophages, T cells, NKs, and DCs, and can also promote T cell adhesion to endothelial cells, antitumor activity, and inhibition of bone marrow colony formation and angiogenesis [53,54,55]. Intriguingly, a high level of serum CXCL10 is associated with severe arthritic disease in humans [14]. In line with exacerbated joint inflammation, CXCL10 expression was selectively up-regulated in Sting-deficient mice compared to WT (**Fig.2**), suggesting a role for CXCL10 in immunopathology following arthritogenic alphavirus infection. CXCL10 is secreted by several cell types including monocytes, endothelial cells, and fibroblasts. Its expression is increased in many kinds of chronic inflammatory arthritis, especially in rheumatoid arthritis (RA), and is highly induced in CHIKV-infected joints and sustained even after peak viral replication (**Fig.2**). It is thus plausible that during CHIKV infection CXCL10 plays a role in leukocyte homing to inflamed tissues and in perpetuation of inflammation, and therefore, tissue damage. Indeed, joint inflammation was alleviated in *Cxcl10*$^{-/-}$ mice (**Fig.3, 4**), and this was accompanied by a significant reduction in macrophages, which constituted the largest immune cell population in joints following infection (**Fig.5 B**) [30,51,56]. These activated macrophages could be a main cellular reservoir for CHIKV persistence during the late stages of infection [30,51] and contribute to sustained inflammation. In addition to recruiting immune cells, CXCL10 signaling could directly stimulate viral replication, for instance, human immunodeficiency virus 1 (HIV-1) replication in macrophages and lymphocytes [57]. In this study, we unexpectedly observed a reduction in CHIKV/ONNV in *Cxcl10*$^{-/-}$ compared to WT mouse feet at the late stages (days 4/6 and thereafter respectively) (**Fig.3 B**, **Fig.4 B**), suggesting a pro-

221 viral role for CXCL10 signaling. However, the absence of CXCL10 did not impact viremia (**Fig.3**
222 **A**), suggesting that CXCL10 signaling is dispensable for systemic viral dissemination. Thus, a
223 reduction of viral loads in *Cxcl10*$^{-/-}$ mouse feet could be due to fewer macrophages that are
224 supportive of viral replication in *Cxcl10*$^{-/-}$ than WT feet [30,51]. Intriguingly, the viral RNA loads in
225 macrophages and neutrophils of *Cxcl10*$^{-/-}$ mouse feet were ~3-6-fold lower than those of WT
226 mice (**Fig.6**). Macrophages and neutrophils were the predominant immune cell types in mouse
227 feet following alphaviral infection (**Fig.5**). As such, it is plausible that CXCL10 signaling could
228 directly promote alphaviral replication in macrophages and/or other immune cells.

229 CXCL10 is also a chemoattractant for CD4^{+} T cells, which, though constituting only a
230 small fraction of immune infiltrates during the second peak of foot swelling, are believed to
231 underlie CHIKV-induced inflammation in mice [16,28,58]. However, CD4^{+} T cells were recruited to
232 footpads by day 6 following ONNV infection and the numbers of CD4^{+} T cells in *Cxcl10*$^{-/-}$ feet
233 were no different than those in WT feet (data not shown).

234 In summary, our results demonstrate that STING signaling suppresses alphaviral
235 replication and pathogenesis of alphavirus-induced arthritis; while CXCL10 signaling does the
236 opposite. Future work is required to elucidate how CXCL10 signaling facilitates alphaviral
237 replication and test if blockade of CXCL10 signaling mitigates alphaviral arthritis.

238

239

Materials and Methods

Mice

All the mice used in this study were purchased and bred in our state-of-art animal facility. Wild-type C57BL/6J (JAX Stock #: 000664), *Cxcl10*$^{-/-}$ (JAX Stock #: 000687 on C57BL/6 background) and Sting mutant (*Sting*$^{gt/gt}$ on C57BL/6 background, JAX Stock #: 017537) mice were obtained from the Jackson Laboratory. For each experiment, both sex (both gender)- and age (range 6-12 weeks)-matched WT/mutant mice were used. Mouse experiments were approved and performed according to the guidelines of the Institutional Animal Care and Use Committee at the University of Connecticut and Yale University.

Cells and Viruses

Vero cells (monkey kidney epithelial cells, Cat. # CCL-81) were purchased from ATCC (Manassas, VA, USA). The cells were grown at 37˚C and 5% CO_2 in complete DMEM medium: Dulbecco's modified Eagle medium (DMEM) (Corning) supplemented with 10% fetal bovine serum (FBS) (Gibco) and 1% penicillin-streptomycin (P/S; Corning). The CHIKV French La Reunion strain LR2006-OPY1 was a kind gift of The Connecticut Agricultural Experiment Station at New Haven, CT, USA. The ONNV non-recombinant strain was provided by the World Reference Center for Emerging Viruses and Arboviruses (WRCEVA) at University of Texas Medical Branch. Both viruses were propagated in Vero cells.

Plaque forming assay

Quantification of infectious viral particles in cell culture supernatants/mouse tissue homogenates/mouse sera was performed on a Vero cell monolayer in a 6-well plate following an established protocol [59]. A serial of 10-fold dilutions of viral samples were prepared in DMEM without fetal bovine serum. In a 6-well plate, 500µL of diluted samples were added to Vero monolayer. The plate was incubated at 37°C and 5% CO_2 for 2 hrs. The inoculum was then

266 removed and replaced with 2 mL of complete DMEM medium with 1% SeaPlaque agarose
267 (Lonza, Cat# 50100). The plate was incubated at 37°C and 5% CO_2 for 3 days, and plaques
268 were visualized by a Neutral Red exclusion assay. Viable cells took up neutral red; while dead
269 cells excluded it and thus formed a circular white spot.
270
271 *Mouse infection and disease monitoring*
272 Age- and sex-matched mice were inoculated subcutaneously in the hind footpad with $3x10^5$
273 plaque forming units (PFUs) of CHIKV/ONNV. Mice were monitored for clinical signs of disease
274 afterwards. Footpad swelling was measured using a precision digital caliper.
275
276 *Histology studies*
277 Mice were sacrificed and feet were removed and fixed with 4% paraformaldehyde. Tissues were
278 embedded in paraffin and were processed to obtain 5µm sections. Tissues were stained with
279 hematoxylin and eosin. Arthritic disease was arbitrarily scored 1-5, with 5 representing the worst,
280 based on exudation of fibrin and inflammatory cells into the joints, alteration in the thickness of
281 tendons or ligament sheaths, and hypertrophy and hyperplasia of the synovium [53]. Slides were
282 imaged using an Accu-Scope EXI-310 model inverted microscope with Infinity Capture software.
283
284 *Flow cytometry and florescence activated cell sorting*
285 Mice were euthanized, footpads and ankles were harvested at 0, 2, 4 and 6 days post infection
286 (dpi). The footpads were skinned and put into 4 ml of digestion medium with 20 mg/ml
287 collagenase IV (Sigma-Aldrich), 5 U/ml dispase (Stemcell) and 50 mg/ml DNase I mix (Qiagen)
288 in complete RPMI1640 medium. The tissues were harvested and incubated in digestion medium
289 on a shaker at 37°C for 4 hrs. The mixture was transferred to a 40µm cell strainer sitting on a
290 collection tube. 5 ml of complete RPMI medium was added to the cell strainer. Using a circular
291 motion, the digested tissues were ground into the medium against the cell strainer to release

maximum number of cells. Cells were then centrifuged at 500xg for 5 min. The supernatant was discarded and red blood cells were lysed using 0.2% sodium chloride. Cells were washed once in complete RPMI medium, re-suspended in 10ml of complete RPMI medium in a 15ml-tube. 10ml of 35% v/v Percoll/RPMI medium was carefully added to the cell suspension. The tube was spun for 20 min at 1200xg. The pellet was re-suspended and washed with complete RPMI medium once.

The isolated cells were then stained for 30 min at 4°C with the following antibodies (Biolegend): APC-Fire 750-anti CD11b (Cat. # 101261), Alexa Flour 700-anti Ly-6G (Cat. # 127621), Brilliant Violet 421-anti CD11c (Cat. # 117343), PerCP-Cy5.5-anti MHC II (Cat. # 107625), PE-anti Tetherin (PCDA1) (Cat. # 12703), Brilliant Violet 510-anti F4/80 (Cat. # 123135), APC-anti CD68 (Cat. # 137007), PE-Dazzle 594-anti CD3 epsilon (Cat. # 100347), Brilliant Violet 711-anti CD4 (Cat. # 100557), Brilliant Violet 570-anti CD8a (Cat. # 100739), FITC-anti CD25 (Cat. # 102005), Zombie UV (Cat. # 423107), PE-Cy7-anti CD45 (Cat. # 103113), TruStain FcX-anti CD16/32 (Cat. # 101319). After staining and washing, the cells were fixed with 4%PFA analyzed by FACS.

Flow cytometry was later performed on a Becton-Dickinson FACS ARIA II, CyAn advanced digital processor (ADP) and analyzed using FlowJo software. Neutrophils were classified as $CD11b^+$ $Ly6G^+$. Macrophage were classified as $CD11b^+$ $F4/80^+$. DC cells were classified as $CD11c^+$ MHC II^+. pDC cells were classified as $CD11c^+$ $PCDA1^+$.

Real-time quantitative RT-PCR

RNA was isolated from blood samples and footpad tissues using a RNAasy mini-prep kit (Invitrogen). For paraformaldehyde-fixed and sorted cells, RNA was isolated using RNeasy FFPE Kit (Qiagen). Isolated RNA was resuspended in RNAse/DNAse free H_2O (Invitrogen) and stored at 4˚C overnight or -80˚C. RT was performed on a Bio-Rad CFX machine using the RNA RT Kit (Takara) with a 10µl total reaction volume per well containing 3µl of RNA samples.

Quantitative PCR (qPCR) was performed with gene specific primers and SYBR Green. The primers for CHIKV were forward primer (5'-GCGAATTCGGCGCAGCACCAAGGACAACTTCA-3') and reverse primer (5'-AATGCGGCCGCCTAGCAGCATATTAGGCTAAGCAGG-3'). The primers for ONNV were forward primer (5'-GCAGGGAGGCCAGGACAGT-3)' and reverse primer (5'-GCCCCTTTTTCYTTGAGCCAGTA-3'). The housekeeping gene control used were beta actin, *Actb*. The following PCR cycling program was used: 10 min at 95˚, and 40 cycles of 15 sec at 95˚ and 1 min at 60˚C. The results were calculated using the -ΔΔCt method.

Statistical analysis

All data were analyzed with GraphPad Prism software. For viral RNA analysis, immune cell analysis, cytokines and chemokines analysis and footpad swelling, data were analyzed by the nonparametric Mann-Whitney test, two-tailed Student's *t* test or multiple t-tests depending on the data distribution and the number of comparison groups. P values of less than 0.05 were considered statistically significant.

345

References

1 Robinson, M. C. An epidemic of virus disease in Southern Province, Tanganyika Territory, in 1952-53. I. Clinical features. *Trans R Soc Trop Med Hyg* **49**, 28-32, doi:10.1016/0035-9203(55)90080-8 (1955).

2 Silva, L. A. & Dermody, T. S. Chikungunya virus: epidemiology, replication, disease mechanisms, and prospective intervention strategies. *J Clin Invest* **127**, 737-749, doi:10.1172/JCI84417 (2017).

3 Weaver, S. C. & Lecuit, M. Chikungunya virus and the global spread of a mosquito-borne disease. *N Engl J Med* **372**, 1231-1239, doi:10.1056/NEJMra1406035 (2015).

4 Weaver, S. C. & Lecuit, M. Chikungunya Virus Infections. *N Engl J Med* **373**, 94-95, doi:10.1056/NEJMc1505501 (2015).

5 Sourisseau, M. *et al.* Characterization of reemerging chikungunya virus. *PLoS Pathog* **3**, e89, doi:10.1371/journal.ppat.0030089 (2007).

6 Krejbich-Trotot, P. *et al.* Chikungunya virus mobilizes the apoptotic machinery to invade host cell defenses. *FASEB J* **25**, 314-325, doi:10.1096/fj.10-164178 (2011).

7 Dhanwani, R., Khan, M., Alam, S. I., Rao, P. V. & Parida, M. Differential proteome analysis of Chikungunya virus-infected new-born mice tissues reveal implication of stress, inflammatory and apoptotic pathways in disease pathogenesis. *Proteomics* **11**, 1936-1951, doi:10.1002/pmic.201000500 (2011).

8 Teng, T. S. *et al.* A Systematic Meta-analysis of Immune Signatures in Patients With Acute Chikungunya Virus Infection. *J Infect Dis* **211**, 1925-1935, doi:10.1093/infdis/jiv049 (2015).

9 Ruiz Silva, M., van der Ende-Metselaar, H., Mulder, H. L., Smit, J. M. & Rodenhuis-Zybert, I. A. Mechanism and role of MCP-1 upregulation upon chikungunya virus infection in human peripheral blood mononuclear cells. *Scientific reports* **6**, 32288, doi:10.1038/srep32288 (2016).

10 Her, Z. *et al.* Active infection of human blood monocytes by Chikungunya virus triggers an innate immune response. *J Immunol* **184**, 5903-5913, doi:10.4049/jimmunol.0904181 (2010).

11 Schilte, C. *et al.* Type I IFN controls chikungunya virus via its action on nonhematopoietic cells. *J Exp Med* **207**, 429-442, doi:10.1084/jem.20090851 (2010).

12 Wauquier, N. *et al.* The acute phase of Chikungunya virus infection in humans is associated with strong innate immunity and T CD8 cell activation. *J Infect Dis* **204**, 115-123, doi:10.1093/infdis/jiq006 (2011).

13 Chang, A. Y. *et al.* Chikungunya Arthritis Mechanisms in the Americas: A Cross-Sectional Analysis of Chikungunya Arthritis Patients Twenty-Two Months After Infection Demonstrating No Detectable Viral Persistence in Synovial Fluid. *Arthritis Rheumatol* **70**, 585-593, doi:10.1002/art.40383 (2018).

14 Kelvin, A. A. *et al.* Inflammatory cytokine expression is associated with chikungunya virus resolution and symptom severity. *PLoS Negl Trop Dis* **5**, e1279, doi:10.1371/journal.pntd.0001279 (2011).

15 Rudd, P. A. *et al.* Interferon response factors 3 and 7 protect against Chikungunya virus hemorrhagic fever and shock. *J Virol* **86**, 9888-9898, doi:10.1128/JVI.00956-12 (2012).

16 Poo, Y. S. *et al.* Multiple immune factors are involved in controlling acute and chronic chikungunya virus infection. *PLoS Negl Trop Dis* **8**, e3354, doi:10.1371/journal.pntd.0003354 (2014).

17 Couderc, T. *et al.* A mouse model for Chikungunya: young age and inefficient type-I interferon signaling are risk factors for severe disease. *PLoS Pathog* **4**, e29, doi:10.1371/journal.ppat.0040029 (2008).

18 Akahata, W. *et al.* A virus-like particle vaccine for epidemic Chikungunya virus protects nonhuman primates against infection. *Nat Med* **16**, 334-338, doi:10.1038/nm.2105 (2010).

19 Fric, J., Bertin-Maghit, S., Wang, C. I., Nardin, A. & Warter, L. Use of human monoclonal antibodies to treat Chikungunya virus infection. *J Infect Dis* **207**, 319-322, doi:10.1093/infdis/jis674 (2013).

20 Prow, T. W. *et al.* Nanopatch-targeted skin vaccination against West Nile Virus and Chikungunya virus in mice. *Small* **6**, 1776-1784, doi:10.1002/smll.201000331 (2010).

21 Wang, D. *et al.* A complex adenovirus vaccine against chikungunya virus provides complete protection against viraemia and arthritis. *Vaccine* **29**, 2803-2809, doi:10.1016/j.vaccine.2011.01.108 (2011).

22 Goh, L. Y. *et al.* Neutralizing monoclonal antibodies to the E2 protein of chikungunya virus protects against disease in a mouse model. *Clin Immunol* **149**, 487-497, doi:10.1016/j.clim.2013.10.004 (2013).

23 Metz, S. W. *et al.* Effective chikungunya virus-like particle vaccine produced in insect cells. *PLoS Negl Trop Dis* **7**, e2124, doi:10.1371/journal.pntd.0002124 (2013).

24 Selvarajah, S. *et al.* A neutralizing monoclonal antibody targeting the acid-sensitive region in chikungunya virus E2 protects from disease. *PLoS Negl Trop Dis* **7**, e2423, doi:10.1371/journal.pntd.0002423 (2013).

25 Pal, P. *et al.* Development of a highly protective combination monoclonal antibody therapy against Chikungunya virus. *PLoS Pathog* **9**, e1003312, doi:10.1371/journal.ppat.1003312 (2013).

26 Fox, J. M. & Diamond, M. S. Immune-Mediated Protection and Pathogenesis of Chikungunya Virus. *J Immunol* **197**, 4210-4218, doi:10.4049/jimmunol.1601426 (2016).

27 Teo, T. H., Lum, F. M., Lee, W. W. & Ng, L. F. Mouse models for Chikungunya virus: deciphering immune mechanisms responsible for disease and pathology. *Immunol Res* **53**, 136-147, doi:10.1007/s12026-012-8266-x (2012).

28 Teo, T. H. *et al.* A pathogenic role for CD4+ T cells during Chikungunya virus infection in mice. *J Immunol* **190**, 259-269, doi:10.4049/jimmunol.1202177 (2013).

29 Gasque, P., Couderc, T., Lecuit, M., Roques, P. & Ng, L. F. Chikungunya virus pathogenesis and immunity. *Vector Borne Zoonotic Dis* **15**, 241-249, doi:10.1089/vbz.2014.1710 (2015).

30 Hoarau, J. J. *et al.* Persistent chronic inflammation and infection by Chikungunya arthritogenic alphavirus in spite of a robust host immune response. *J Immunol* **184**, 5914-5927, doi:10.4049/jimmunol.0900255 (2010).

31 Petitdemange, C. *et al.* Unconventional repertoire profile is imprinted during acute chikungunya infection for natural killer cells polarization toward cytotoxicity. *PLoS Pathog* **7**, e1002268, doi:10.1371/journal.ppat.1002268 (2011).

32 Stoermer, K. A. *et al.* Genetic ablation of arginase 1 in macrophages and neutrophils enhances clearance of an arthritogenic alphavirus. *J Immunol* **189**, 4047-4059, doi:10.4049/jimmunol.1201240 (2012).

33 Ishikawa, H. & Barber, G. N. STING is an endoplasmic reticulum adaptor that facilitates innate immune signalling. *Nature* **455**, 674-678, doi:10.1038/nature07317 (2008).

34 Ishikawa, H., Ma, Z. & Barber, G. N. STING regulates intracellular DNA-mediated, type I interferon-dependent innate immunity. *Nature* **461**, 788-792, doi:10.1038/nature08476 (2009).

35 Zhong, B. *et al.* The adaptor protein MITA links virus-sensing receptors to IRF3 transcription factor activation. *Immunity* **29**, 538-550, doi:10.1016/j.immuni.2008.09.003 (2008).

36 Sun, W. *et al.* ERIS, an endoplasmic reticulum IFN stimulator, activates innate immune signaling through dimerization. *Proceedings of the National Academy of Sciences of the United States of America* **106**, 8653-8658, doi:10.1073/pnas.0900850106 (2009).

37 Wu, J. *et al.* Cyclic GMP-AMP is an endogenous second messenger in innate immune signaling by cytosolic DNA. *Science* **339**, 826-830, doi:10.1126/science.1229963 (2013).

38 Sun, L., Wu, J., Du, F., Chen, X. & Chen, Z. J. Cyclic GMP-AMP synthase is a cytosolic DNA sensor that activates the type I interferon pathway. *Science* **339**, 786-791, doi:10.1126/science.1232458 (2013).

39 Burdette, D. L. *et al.* STING is a direct innate immune sensor of cyclic di-GMP. *Nature* **478**, 515-518, doi:10.1038/nature10429 (2011).

40 Li, X. D. *et al.* Pivotal roles of cGAS-cGAMP signaling in antiviral defense and immune adjuvant effects. *Science* **341**, 1390-1394, doi:10.1126/science.1244040 (2013).

41 Nazmi, A., Mukhopadhyay, R., Dutta, K. & Basu, A. STING mediates neuronal innate immune response following Japanese encephalitis virus infection. *Scientific reports* **2**, 347, doi:10.1038/srep00347 (2012).

42 You, F. *et al.* ELF4 is critical for induction of type I interferon and the host antiviral response. *Nature immunology* **14**, 1237-1246, doi:10.1038/ni.2756 (2013).

43 Chen, H. *et al.* Activation of STAT6 by STING is critical for antiviral innate immunity. *Cell* **147**, 436-446, doi:10.1016/j.cell.2011.09.022 (2011).

44 Liu, Y. *et al.* RIG-I-Mediated STING Upregulation Restricts Herpes Simplex Virus 1 Infection. *J Virol* **90**, 9406-9419, doi:10.1128/JVI.00748-16 (2016).

45 Holm, C. K. *et al.* Virus-cell fusion as a trigger of innate immunity dependent on the adaptor STING. *Nat Immunol* **13**, 737-743, doi:10.1038/ni.2350 (2012).

46 Franz, K. M., Neidermyer, W. J., Tan, Y. J., Whelan, S. P. J. & Kagan, J. C. STING-dependent translation inhibition restricts RNA virus replication. *Proc Natl Acad Sci U S A* **115**, E2058-E2067, doi:10.1073/pnas.1716937115 (2018).

47 Sharma, S. *et al.* Suppression of systemic autoimmunity by the innate immune adaptor STING. *Proc Natl Acad Sci U S A* **112**, E710-717, doi:10.1073/pnas.1420217112 (2015).

48 Sauer, J. D. *et al.* The N-ethyl-N-nitrosourea-induced Goldenticket mouse mutant reveals an essential function of Sting in the in vivo interferon response to Listeria monocytogenes and cyclic dinucleotides. *Infect Immun* **79**, 688-694, doi:10.1128/IAI.00999-10 (2011).

49 Persson, T. *et al.* Expression of the neutrophil-activating CXC chemokine ENA-78/CXCL5 by human eosinophils. *Clin Exp Allergy* **33**, 531-537 (2003).

50 Long, K. M. *et al.* gammadelta T Cells Play a Protective Role in Chikungunya Virus-Induced Disease. *J Virol* **90**, 433-443, doi:10.1128/JVI.02159-15 (2015).

51 Labadie, K. *et al.* Chikungunya disease in nonhuman primates involves long-term viral persistence in macrophages. *J Clin Invest* **120**, 894-906, doi:10.1172/JCI40104 (2010).

52 Gardner, J. *et al.* Chikungunya Virus Arthritis in Adult Wild-Type Mice. *J Virol* **84**, 8021-8032, doi:10.1128/Jvi.02603-09 (2010).

53 Angiolillo, A. L. *et al.* Human interferon-inducible protein 10 is a potent inhibitor of angiogenesis in vivo. *J Exp Med* **182**, 155-162 (1995).

54 Dufour, J. H. *et al.* IFN-gamma-inducible protein 10 (IP-10; CXCL10)-deficient mice reveal a role for IP-10 in effector T cell generation and trafficking. *J Immunol* **168**, 3195-3204 (2002).

55 Petrovic-Djergovic, D. *et al.* CXCL10 induces the recruitment of monocyte-derived macrophages into kidney, which aggravate puromycin aminonucleoside nephrosis. *Clin Exp Immunol* **180**, 305-315, doi:10.1111/cei.12579 (2015).

56 Gardner, J. *et al.* Chikungunya virus arthritis in adult wild-type mice. *J Virol* **84**, 8021-8032, doi:10.1128/JVI.02603-09 (2010).

494 57 Lane, B. R. *et al.* The C-X-C chemokine IP-10 stimulates HIV-1 replication. *Virology* **307**,
495 122-134, doi:10.1016/s0042-6822(02)00045-4 (2003).
496 58 Teo, T. H. *et al.* Fingolimod treatment abrogates chikungunya virus-induced arthralgia.
497 *Sci Transl Med* **9**, doi:10.1126/scitranslmed.aal1333 (2017).
498 59 Wang, P. Exploration of West Nile Virus Infection in Mouse Models. *Methods Mol Biol*
499 **1435**, 71-81, doi:10.1007/978-1-4939-3670-0_7 (2016).

500

Acknowledgements

We are grateful to The Connecticut Agricultural Experiment Station for providing Chikungunya virus. This work was supported by a National Institutes of Health grant R01AI132526 to P.W.

Author contributions

T.L. and T.G designed and performed the majority of the experimental procedures and data analyses. A.H. and D.Y. contributed to some of the experiments and/or provided technical support. A.V. and E.F. helped with data interpretations and writing. P.W. conceived and oversaw the study. T.L. and P.W. wrote the paper and all the authors reviewed and/or modified the manuscript.

Conflict of Interest

The authors declare no competing financial/non-financial interest.

FIGURE LEGENDS

Fig.1 CHIKV pathogenesis is exacerbated in *Sting*$^{gt/gt}$ mice. Age- and sex-matched, C57BL/6 (WT) and STING deficient (*Sting*$^{gt/gt}$) mice were infected with CHIKV. **A**) quantitative RT-PCR (qPCR) quantification of CHIKV loads in whole blood cells. **B**) Viremia of day 2 sera quantified by plaque forming assay (PFU/ml serum). qPCR analysis of CHIKV loads in **C**) the spleen and **D**) ankle joints. **E**) Viral titers in footpads on day 4 pi (PFU/gram tissue). **F**) Fold changes in the footpad dimensions of infected (days 0.5, 1, 4, 6 and 8) over the uninfected (day 0) (N=4-6 per experimental group). **G**) Arbitrary scores of day 8 ankle joint inflammation and damage using a scale 1 to 5, with 5 representing the worst disease presentation. Each dot represents one mouse; the small horizontal line indicates the median of the result. N=6/genotype. **H**) Representative H&E micrographs of footpad inflammation 8 days after infection. N=6/genotype. Magnifications 40x. B: bone, T: tendon, M: muscle. Boxed areas indicate the regions with severe infiltration and tissue damage. Magnification: 200x. The data represent two independent experiments. *, P<0.05; **, p<0.01; ***, P<0.001 [**A-E**) non-parametric Mann-Whitney U test, **F** and **G**)] two-tailed Student's t-test].

Fig.2 STING deficiency selectively elevates expression of CXCL10 in ankle joints. Age- and sex-matched, C57BL/6 (WT) and STING deficient (*Sting*$^{gt/gt}$) mice were infected with CHIKV. **A**) Multiple genes are differentially expressed in the joints of *Sting*$^{gt/gt}$ (N=6) vs. WT (N=8) mice at day 8 p.i. by PCR array. **B**) qPCR analysis of gene expression at various time points after infection. Each dot=one mouse. The horizontal line in each column=the median. *, P<0.05; **, P<0.01; ***, P<0.001 (non-parametric Mann-Whitney t test).

552 **Fig.3 CXCL10 signaling facilitates CHIKV pathogenesis in mouse feet.** Age- and sex-
553 matched, C57BL/6 (WT) and Cxcl10 deficient (*Cxcl10*$^{-/-}$) mice were infected with CHIKV. **A**)
554 Quantification of viremia by qPCR in whole blood cells (left panel) and plaque assay (PFU/ml
555 serum) (right panel) of wild type (WT) and *Cxcl10*$^{-/-}$ mice. **B**) Quantification of viral loads by
556 qPCR (left panel) and plaque forming assay (PFU/g tissue, day 7) at various days after
557 infection. **C**) Representative H&E micrographs and arbitrary scores of ankle joint inflammation
558 and damage using a scale 1 to 5, with 5 representing the worst disease at 7 days after CHIKV
559 infection. N=5-6/genotype. Magnifications 40X. B: bone, T: tendon, M: muscle. Boxed areas
560 indicate the regions with infiltration and tissue damage. Magnification: 200x. **D**) qPCR
561 quantification of cytokines in ankle joints at day 8 p.i. Each dot=one mouse. The horizontal line
562 in each column=the median. *, P<0.05; **, P<0.01 [(non-parametric Mann-Whitney t test for **B**)
563 and two-tailed Student's t-test for **D**)].
564
565 **Fig.4 CXCL10 signaling facilitates ONNV pathogenesis in mouse feet.** Age- and sex-
566 matched, C57BL/6 (WT) and Cxcl10 deficient (*Cxcl10*$^{-/-}$) mice were infected with ONNV. **A**)
567 qPCR quantification of ONNV loads in **A**) whole blood cells and **B**) the ankle joints at various
568 days after infection. **C**) Arbitrary scores of ankle joint inflammation and damage using a scale 1
569 to 5, with 5 representing the worst disease at 6 days after ONNV infection. N=6/genotype. Each
570 dot=one mouse. The horizontal line in each column=the median. *, P<0.05; **, P<0.01 [(non-
571 parametric Mann-Whitney t test for **B**) and two-tailed Student's t-test for **C**)].
572
573 **Fig.5 CXCL10 signaling facilitates macrophage infiltration into mouse feet.** Age- and sex-
574 matched, C57BL/6 (WT) and Cxcl10 deficient (*Cxcl10*$^{-/-}$) mice were infected with ONNV.
575 Different immune cells were quantitated by FACS. The frequencies of **A**) total CD45^{+} immune
576 cells, **B**) CD11b^{+} F4/80^{+} macrophages, **C**) CD11b^{+} Ly-6G^{+} neutrophils, **D**) CD11c^{+} MHCII^{+}
577 conventional dendritic cells (cDC), and **E**) CD11c^{+} PCDA1^{+} plasmacytoid dendritic cells (pDC).

578 Each dot=one mouse. The horizontal line in each column=the median. *, P<0.05 (non-
579 parametric Mann-Whitney t test).
580
581 **Fig.6 Viral RNA loads are reduced in *Cxcl10*$^{-/-}$ macrophages and neutrophils**. Age- and
582 sex-matched, C57BL/6 (WT) and Cxcl10 deficient (*Cxcl10*$^{-/-}$) mice were infected with ONNV.
583 Immune cells were sorted by FACS. ONNV RNA in the sorted immune cells was quantitated by
584 RT-PCR. Each dot=one mouse. The horizontal line in each column=the median. P values were
585 calculated with multiple t-tests.

Fig. 1

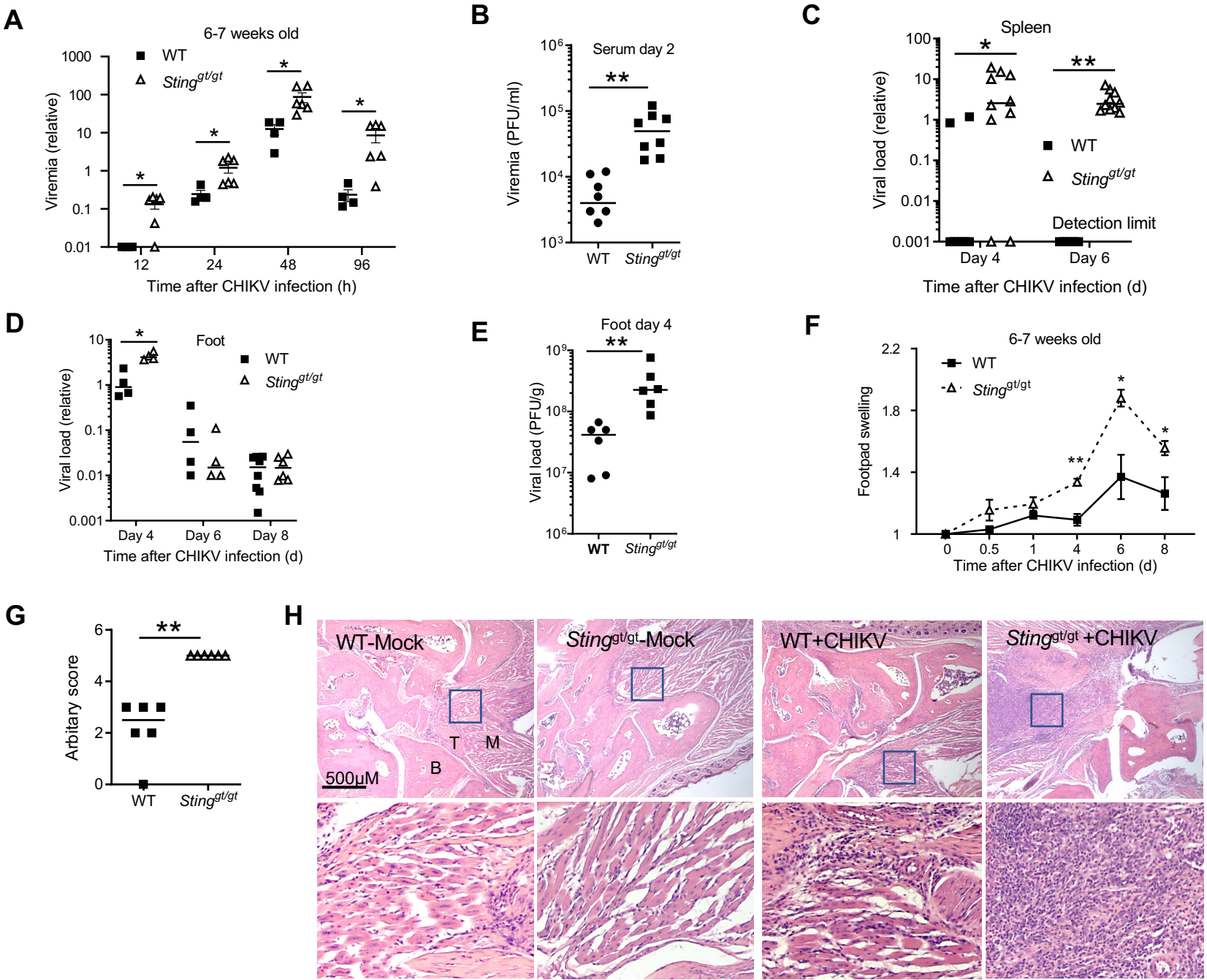
A
6-7 weeks old
WT
Sting gt/gt
Viremia (relative)
Time after CHIKV infection (h)
B
Serum day 2
Viremia (PFU/ml)
C
Spleen
Viral load (relative)
Detection limit
Day 4
Day 6
Time after CHIKV infection (d)
D
Foot
Viral load (relative)
Day 8
E
Foot day 4
Viral load (PFU/g)
F
6-7 weeks old
Footpad swelling
G
Arbitary score
H
WT-Mock
Sting gt/gt -Mock
WT+CHIKV
Sting gt/gt +CHIKV
T
M
B
500μM

Fig. 2

A

Symbol	Fold change	Symbol	Fold change
C5AR1	-1.29	CXCL1	-1.13
ACKR2	-1.43	CXCL10	4.14
CCL1	1.14	CXCL11	1.57
CCL11	1.02	CXCL12	-2.04
CCL12	2.10	CXCL13	-1.42
CCL17	-1.62	CXCL14	-2.54
CCL19	-1.23	CXCL15	-1.20
CCL2	2.63	CXCL16	-1.02
CCL20	-1.26	CXCL2	1.31
CCL22	1.06	CXCL3	-2.11
CCL24	-1.64	CXCL5	-3.35
CCL25	1.15	CXCL9	1.45
CCL26	-1.68	CXCR1	-1.68
CCL28	-1.68	CXCR2	-4.43
CCL3	1.41	CXCR3	-1.02
CCL4	1.78	CXCR4	-1.98
CCL5	1.44	CXCR5	-2.01
CCL6	1.10	CXCR6	1.53
CCL7	1.92	ACKR3	-1.30
CCL8	1.56	ACKR1	-1.37
CCL9	1.08	FPR1	-1.43
CCR1	-1.04	GPR17	-1.68
CCR10	-1.39	HIF1A	-1.11
CCR1L1	-1.68	IFNG	4.92
CCR2	1.46	IL16	-1.54
CCR3	1.39	IL1B	1.19
CCR4	1.29	IL4	-2.62
CCR5	1.37	IL6	-2.05
CCR6	-1.88	ITGAM	-1.09
CCR7	-1.58	ITGB2	-1.17
CCR8	-1.44	MAPK1	-1.17
CCR9	-2.05	MAPK14	-1.36
ACKR4	-2.48	PF4	-1.33
CCRL2	-1.32	PPBP	-5.22
CMKLR1	-1.11	SLIT2	-1.83
CMTM2A	-1.68	TGFB1	-1.46
CMTM3	1.39	TLR2	-1.02
CMTM4	-1.24	TLR4	-1.09
CMTM5	-1.57	TNF	1.22
CMTM6	-1.78	TYMP	-1.25
CX3CL1	-2.14	XCL1	1.24
CX3CR1	-1.23	XCR1	1.40

B

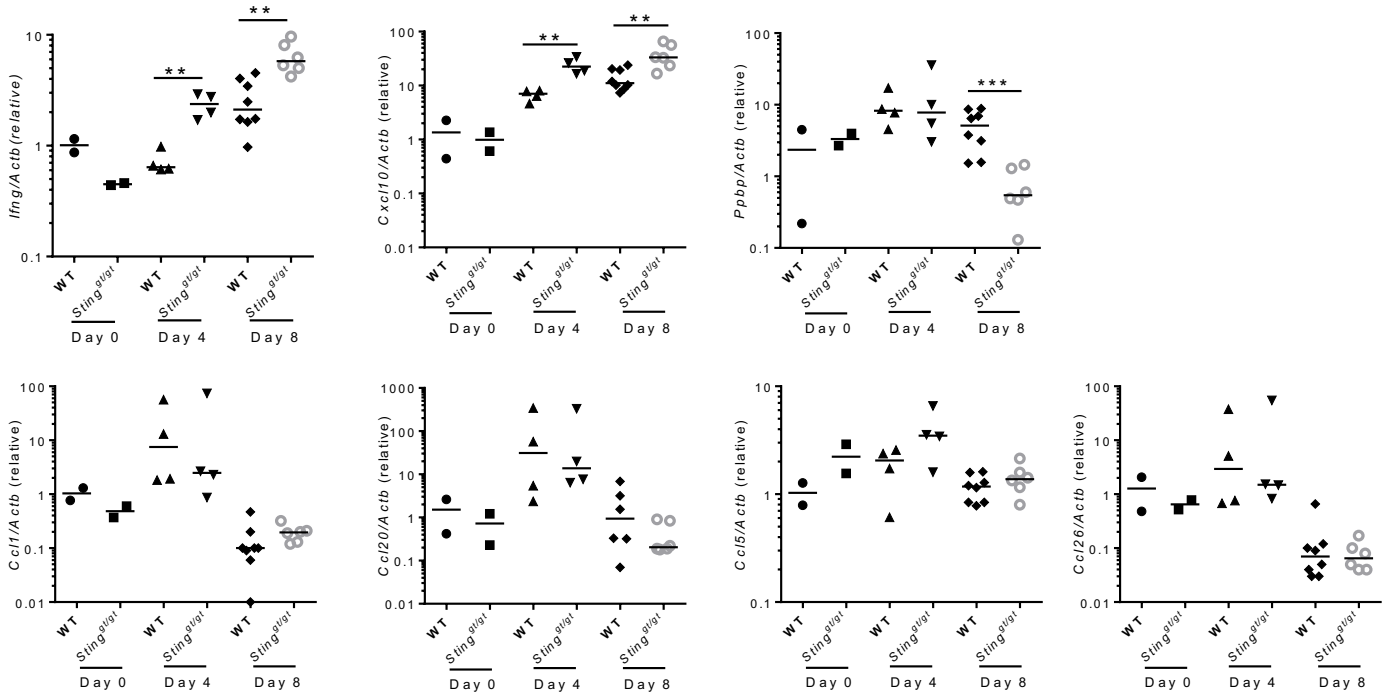

Fig. 3

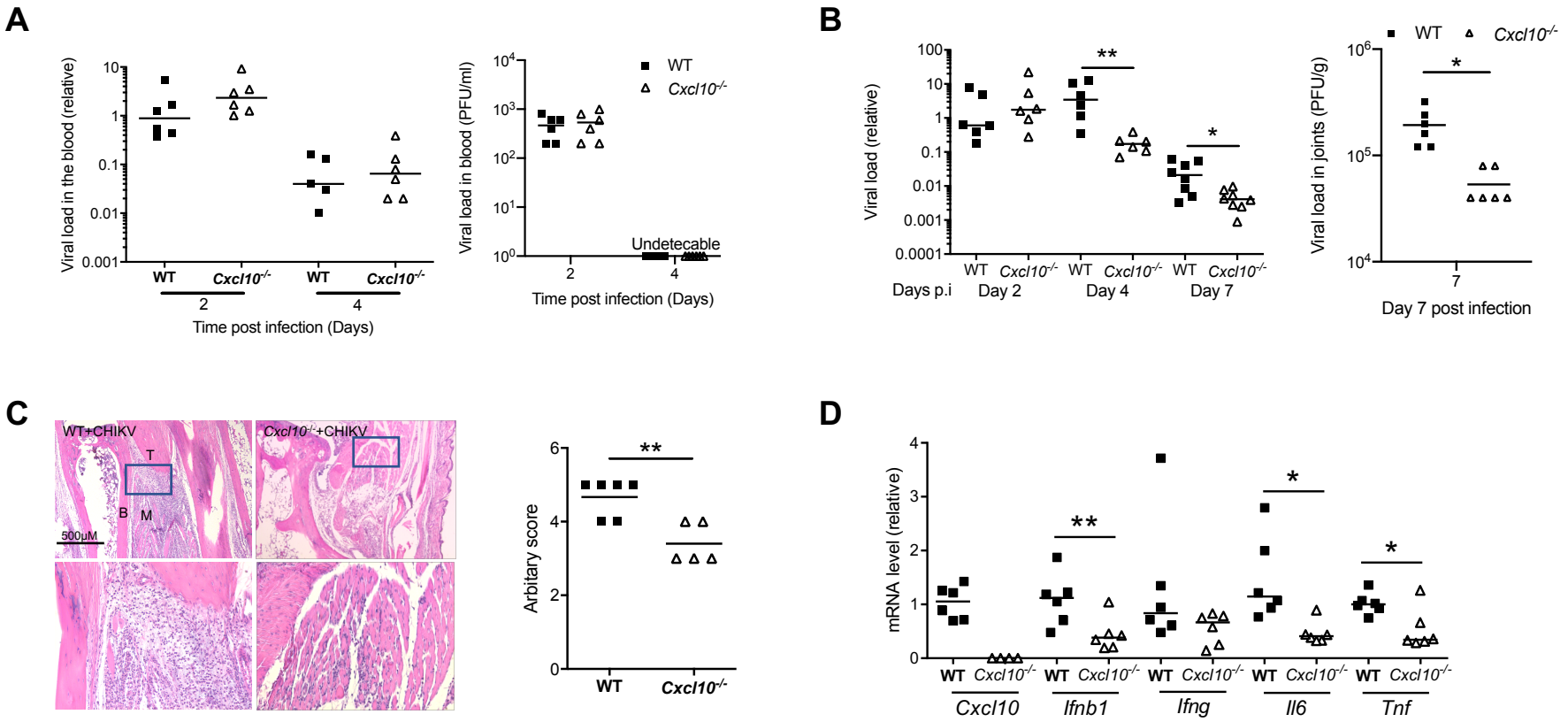
A
Viral load in the blood (relative)
10
1
0.1
0.01
0.001
WT
Cxcl10-/-
WT
Cxcl10-/-
2
4
Time post infection (Days)
Viral load in blood (PFU/ml)
10^4
10^3
10^2
10^1
10^0
WT
Cxcl10-/-
Undetecable
2
4
Time post infection (Days)
B
Viral load (relative)
100
10
1
0.1
0.01
0.001
0.0001
**
*
WT
Cxcl10-/-
WT
Cxcl10-/-
WT
Cxcl10-/-
Days p.i
Day 2
Day 4
Day 7
Viral load in joints (PFU/g)
10^6
10^5
10^4
WT
Cxcl10-/-
*
7
Day 7 post infection
C
WT+CHIKV
Cxcl10-/-+CHIKV
T
B
M
500μM
Arbitary score
6
4
2
0
**
WT
Cxcl10-/-
D
mRNA level (relative)
4
3
2
1
0
**
*
*
WT
Cxcl10-/-
Cxcl10
Ifnb1
Ifng
Il6
Tnf

Fig. 4

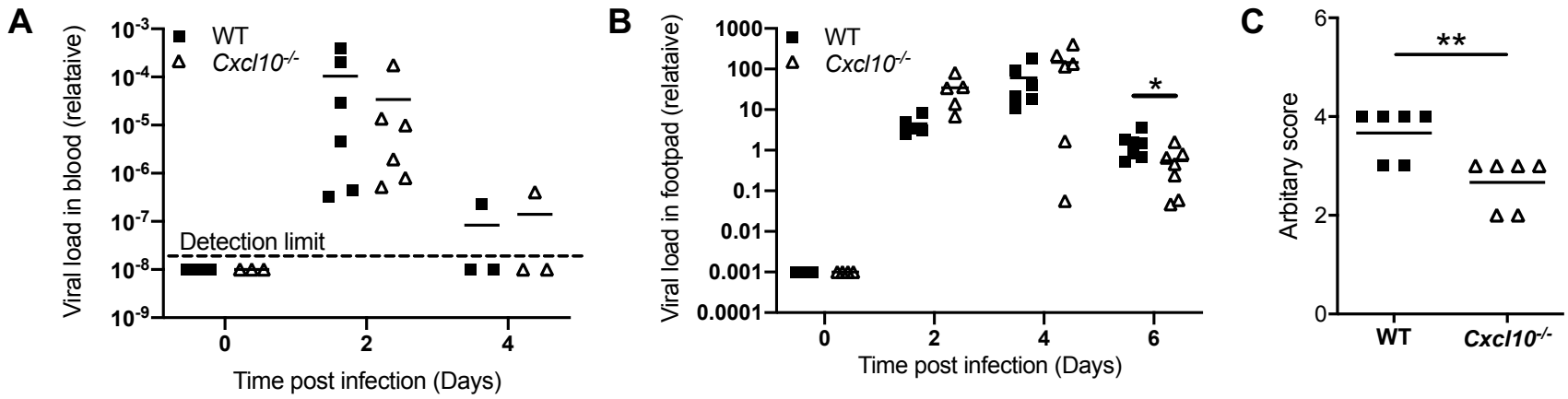
A
Viral load in blood (relataive)
WT
Cxcl10-/-
Detection limit
Time post infection (Days)
B
Viral load in footpad (relataive)
WT
Cxcl10-/-
*
Time post infection (Days)
C
Arbitary score
**
WT
Cxcl10-/-

Fig. 5

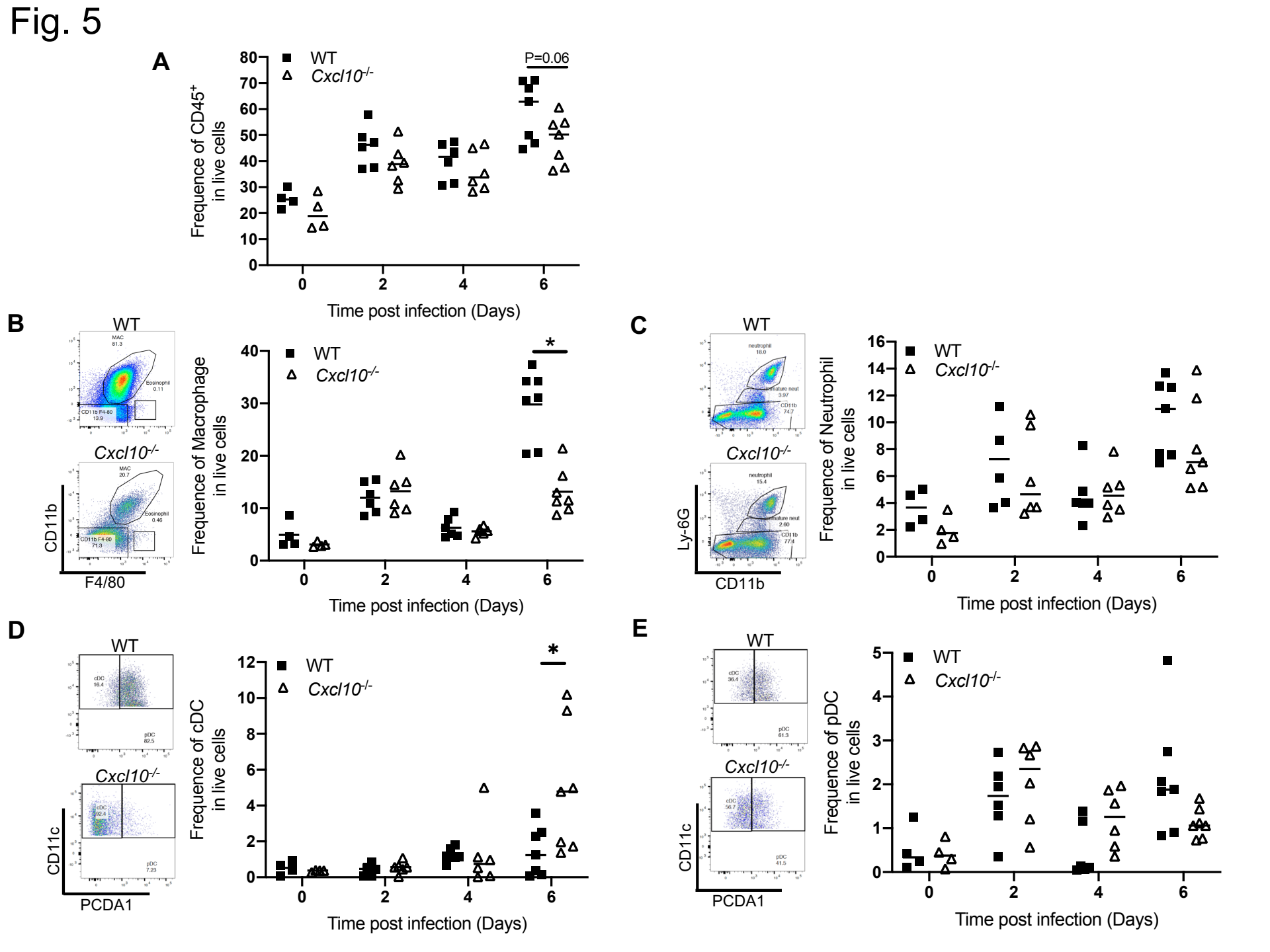
A
WT
Cxcl10-/-
P=0.06
Frequence of CD45+ in live cells
Time post infection (Days)
B
WT
Cxcl10-/-
CD11b
F4/80
Frequence of Macrophage in live cells
*
Time post infection (Days)
C
WT
Cxcl10-/-
Ly-6G
CD11b
Frequence of Neutrophil in live cells
Time post infection (Days)
D
WT
Cxcl10-/-
CD11c
PCDA1
Frequence of cDC in live cells
*
Time post infection (Days)
E
WT
Cxcl10-/-
CD11c
PCDA1
Frequence of pDC in live cells
Time post infection (Days)

Fig. 6

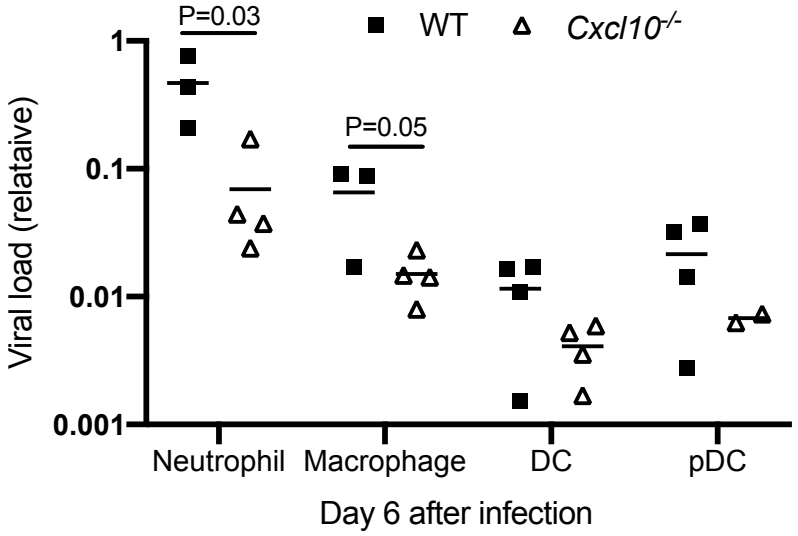
P=0.03
WT
Cxcl10-/-
P=0.05
1
0.1
0.01
0.001
Viral load (relataive)
Neutrophil
Macrophage
DC
pDC
Day 6 after infection